Available online at www.sciencedirect.com

ScienceDirect

Physics Procedia 61 (2015) 138 – 143

Physics Procedia

Status of the XMASS experiment

S. Moriyama for the XMASS collaboration

Kamioka Observatory, Institute for Cosmic Ray Research,
The University of Tokyo, Higashi-Mozumi, Kamioka, Hida, Giu 506-1205, Japan
Kavli Institute for the Physics and Mathematics of the Universe (WPI), The University of Tokyo, Kashiwa, Chiba 277-8582, Japan

Abstract

The goal of the XMASS experiment is direct detection of dark matter using single-phase liquid xenon. The current-phase detector XMASS-I has the largest target mass (835 kg in total) and achieves the lowest energy threshold (300-eV-electron equivalent). The next phase detector XMASS-1.5 will have a total five tons of liquid xenon and is planned to start in 2015. This paper reports results of searches conducted with XMASS-I [low-mass weakly interacting massive particles (WIMPs), solar axions, annual modulation of event rate at low energy, and inelastic scattering of ^{129}Xe nuclei by WIMPs] the current status of hardware modification of XMASS-I to reduce background, and progress in designing XMASS-1.5.

Selection and peer review is the responsibility of the Conference lead organizers, Frank Avignone, University of South Carolina, and Wick Haxton, University of California, Berkeley, and Lawrence Berkeley Laboratory

Keywords: dark matter, xenon, light WIMPs, solar axions, inelastic scattering, super-WIMPs, dark photons

1. XMASS experiment

The XMASS project [1] proposed to use large liquid-xenon detectors to observe rare events such as elastic scattering of electrons by pp solar neutrinos, neutrinoless double-beta decay, and elastic scattering of nuclei by dark matter particles. Liquid xenon is a suitable material for enlarging target mass as well as to obtain low background: xenon gas has no long-living radioisotopes and has high atomic number and high density. With these properties, liquid xenon naturally shields radiation, thereby produce low-background volume. Because liquid xenon is an efficient scintillator, we can reconstruct interaction vertices using, for example, information from photomultipliers arranged around a liquid-xenon target volume. Extracting the events that only happening near the volume center, we can search for rare events in a low-background target mass. Another advantage available with xenon is that techniques exist to reduce contamination in the gas phase. Distillation [2] and active charcoal [3] can be used to remove krypton and radon from xenon gas.

2. XMASS-I and its performance

The first stage of the XMASS project concentrated on the search for dark matter. One candidate for dark matter is weakly interacting massive particles (WIMPs). The XMASS-I detector with 835 kg of liquid xenon (100 kg fiducial mass) was constructed in 2010 and the commissioning run lasted from 2010 to 2012. During the commissioning run, we calibrated the detector and tested its performance. Figure 1 (left) shows calibration data acquired by using a radioactive source ^{57}Co positioned at the center of the detector.

Selection and peer review is the responsibility of the Conference lead organizers, Frank Avignone, University of South Carolina, and Wick Haxton, University of California, Berkeley, and Lawrence Berkeley Laboratory
doi:10.1016/j.phpro.2014.12.023

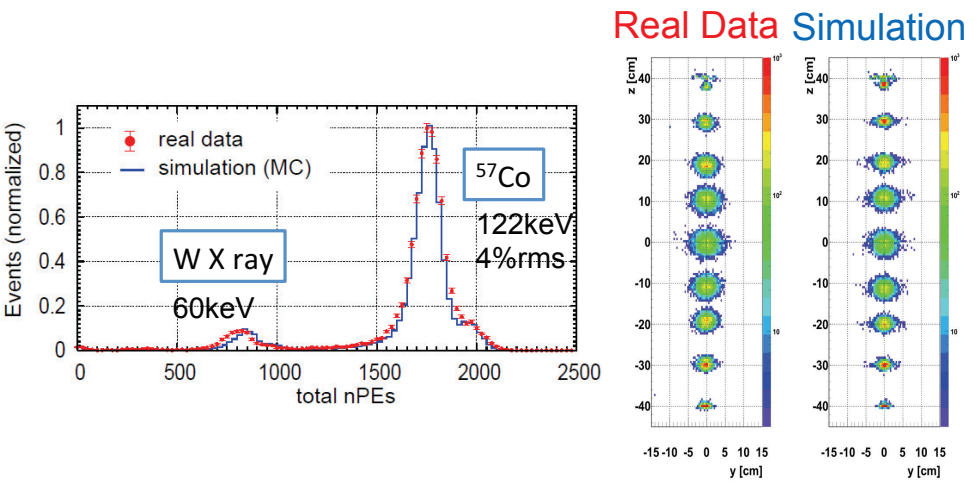

Fig. 1. (Left) Photoelectron distribution for calibration data acquired at detector center. The light yield in our simulation was adjusted to reproduce the peak position of the data. (Right) Overlay of distributions of reconstructed vertices for various position of the radioactive source along the vertical axis of the detector.

From this data, the photoelectron yield was determined to be 14.7 photoelectrons per one keV deposited by 122 keV gamma rays. This is the best light yield among existing detectors for the dark matter search. Figure 1 (right) shows an overlay of distributions of reconstructed vertices for the radioactive source positioned at various positions along the vertical axis of the detector. The experimental distributions are well reproduced by Monte Carlo simulations [4]. Based on these data, we confirmed the detector works as expected.

3. Results of XMASS-I

During the commissioning period, we conducted several searches using the acquired data. Studies of the seasonal modulation with 835 kg of liquid xenon and a fiducial-volume based analysis for heavy WIMPs are ongoing.

3.1. Search for light WIMPs

Since little energy is deposited by light WIMPs [5], the low-energy threshold of our detector is advantageous for detecting them. The 300-eV-electron-equivalent energy threshold of the XMASS-I detector is determined by four hits, which are required to trigger the XMASS-I detector. Without fiducializing we analyzed all events after a cut to reduce Cherenkov events that occur in the quartz windows of photomultiplier tubes (PMTs).

To constrain light WIMPs, we compared the expected energy spectrum for light WIMPs with the observed energy spectrum [Fig. 2 (left)], and set an upper cross-section limit for various WIMP masses [Fig. 2 (right)]. The data were accumulated over 6.7 days with the 835 kg liquid-xenon target.

3.2. Search for solar axions

The strong *CP* problem is a long standing problem in the quantum chromodynamics. The axion is a hypothetical particle predicted by the Pecci–Quinn solution to the problem. The search for axions as well as axion-like particles (ALPs) can be conducted by considering the Sun as a source of these hypothetical particles. Because ALPs should be generated in the core of the Sun, their typical energy of a few keV corresponds to the temperature of the core. These particles can couple to electrons, which causes the axioelectric effect, and deposit their total energy in the XMASS-I detector. To search for such particles, we used the data from the search for light WIMPs. Figure 3 compares the data and with expected spectra for various axion masses [6]. By requiring the expected spectra to not exceed the observed energy spectrum, we limited the axion-electron-electron coupling constant g_{aee}, as shown in Fig. 3 (right).

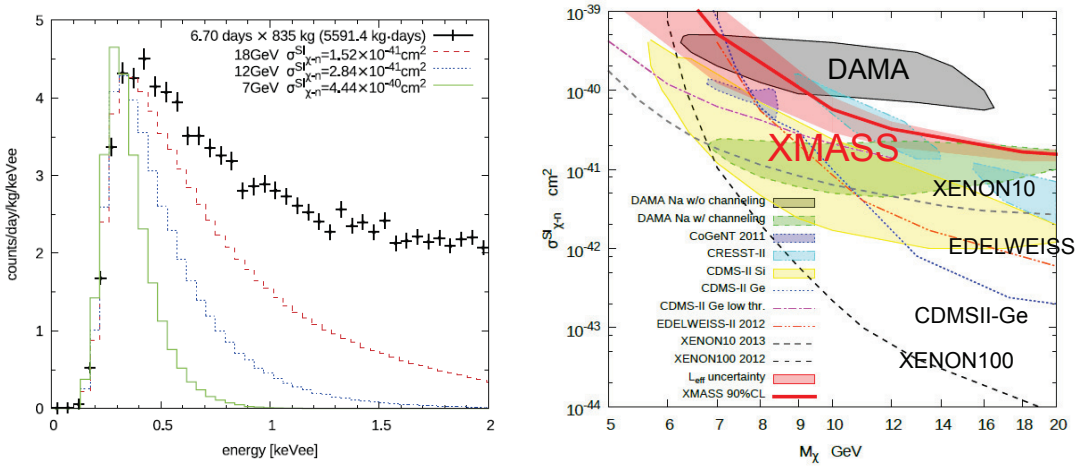

Fig. 2. (Left) Energy distribution of the observed data. The solid, dotted, and dashed lines are expectations for 7, 12, and 18 GeV WIMPs with cross sections indicated in the figure. (Right) Upper limit of the cross section for light WIMPs. The red solid line shows our limit and the band shows the uncertainty of L_{eff}.

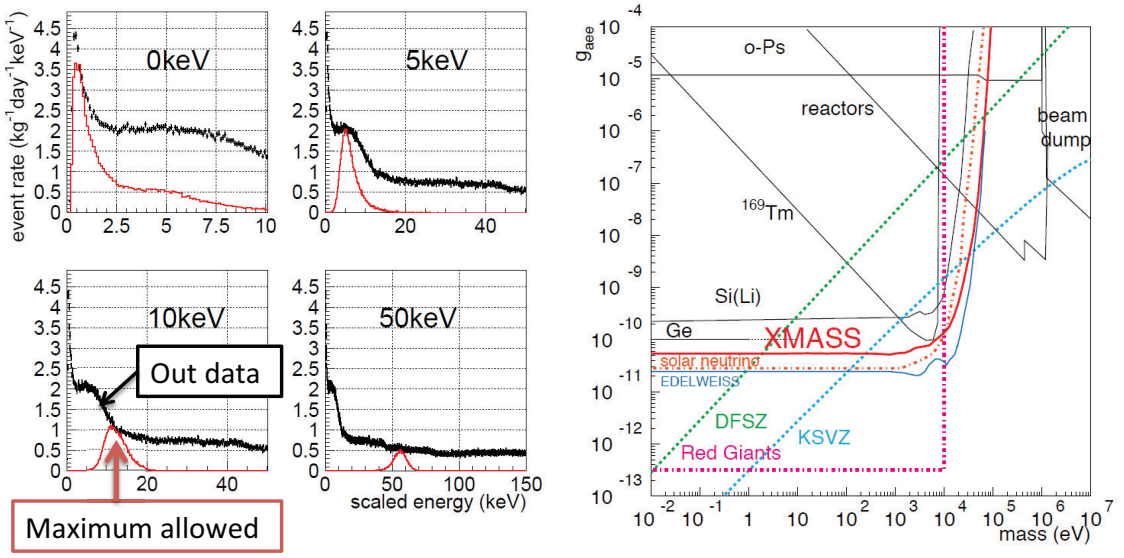

Fig. 3. (Left) Photoelectron distribution for data and expectations for various axion masses. The red histograms show the maximum allowed intensity of axion contributions. (Right) Upper limit on axion electron coupling constant g_{aee}. The red solid line shows our limit, solid lines are from other experimental results, dashed lines are theoretical predictions from axion models, and dot-dashed lines are from astrophysical constraints.

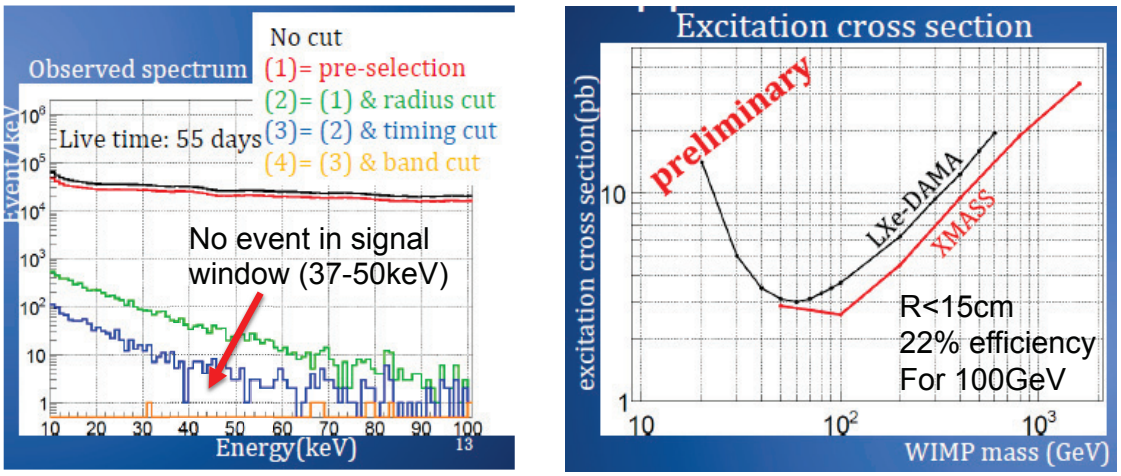

Fig. 4. (Left) Photoelectron distribution for data after each reduction step. No event can be seen in the signal window. (Right) Upper limit on excitation cross section for ^{129}Xe. The red and black lines show our limit and that of a previous experiment. Our low background allows us to derive this limit without background subtraction.

3.3. Inelastic scattering on ^{129}Xe

WIMPs are expected cause inelastic scattering off nuclei as well as elastic scattering. ^{129}Xe has an excited state at 39.58 keV that can be excited by spin-dependent coupling between WIMPs and nucleons [7]. Because the lifetime of the excited state is short (~1 ns), we cannot separate scintillation light from a nuclear recoil or from particles emitted after de-excitation of the excited state. Thus, we expect a peak at 39.58 keV with a high-energy tail.

To make sensitive search for these events, we applied various cuts to reduce the background. These include a standard cut to remove noise and Cherenkov events in the quartz windows of PMTs, a cut based on reconstructed event vertices, a cut based on timing information, and a pattern based cut for rejecting surface events between PMTs. The energy spectra observed after the each step are shown in Fig. 4 (left, 55 days of live-time). Because no events occur in the signal window (37–50 keV), we set an upper limit on the cross section of inelastic scattering. Figure 4 (right) shows the limit as well as the constraint from Ref. [8]. Our background reduction allowed us to derive this limit without explicitly subtracting the remaining events as was done in Ref. [8].

3.4. Vector-boson super-WIMPs

Problems still remain in the cold-dark-matter model. Lighter particles in the keV to MeV region may soften the problem and are proposed in the literature [9, 10]. In Ref. [9], a model referred to as “bosonic super-WIMPs” is discussed. In particular, the vector super-WIMPs in this mass range are not experimentally constrained and are a good candidate for thermally generated dark matter in the Universe. Interestingly, the bosonic nature of the particles means that their total energy is deposited including their rest mass when they are absorbed in the target material. With these characteristics, we can expect the energy spectrum to have a monochromatic peak at their rest mass that can be easily discriminated from the background.

The data set and reduction method used to search for inelastic scattering from ^{129}Xe was used in this search. For the various rest masses of the vector super-WIMPs, we optimized the cut parameters in the reduction steps so as to obtain the best sensitivity. We applied the optimized reduction to our data and to Monte Carlo event samples and compared them to extract a signal from our data. We observed no signal but did obtain a constraint (see Fig. 7). This is the first experimental result that constrains the electron coupling of bosonic super-WIMPs in 40 to 80 keV of its rest mass.

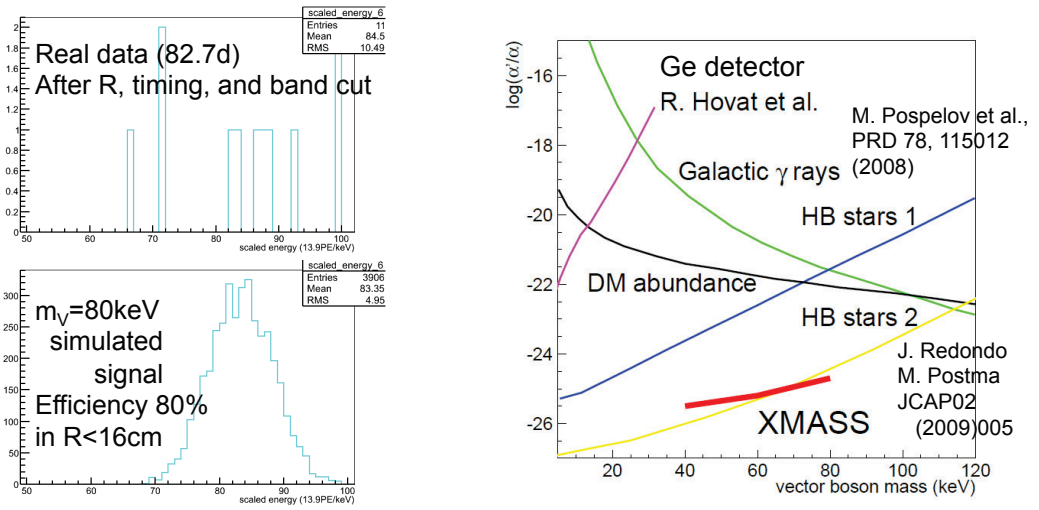

Fig. 5. (Left) Photoelectron distribution for data and expectations for vector super-WIMPs with mass of 80 keV after applying reduction. (Right) Upper limit on fine structure constant of vector boson α' relative to fine structure constant of electromagnetic force α. The red and black lines show our limit and the prediction for dark matter which predicts $\Omega_{DM} = 0.2$. The yellow and blue lines are the constraints by the arguments with horizontal branch stars and the green line shows the constraint based on diffuse gamma rays in the Universe. The purple line shows the experimental constraint obtained from a germanium detector.

4. Refurbishment of XMASS-I

In our study of the background, we found that the aluminum seal of the PMT entrance windows was causing the majority of observed events. However, some other candidates for these events were also identified. To confirm our understanding and to reduce the background, we devised a plan to refurbish the detector. To shield radiations and scintillation lights caused by the aluminum seal, we covered PMTs with copper rings as shown in Fig. 6 (left). Thin copper plates were used to cover gaps between the rings so that scintillation light emitted between the gaps could not diffuse into a sensitive volume (right). Electro polish was applied to the surface of the copper rings and plates to minimize radon daughter nuclei on the surface. The refurbishment work is almost finished and data acquisition is expected to resume in fall of 2013.

Fig. 6. (Left) Copper ring for shield from radiation and scintillation light caused by radioactivity in aluminum seal between PMT window and PMT body. (Right) Thin copper plates to cover gaps between copper rings of PMTs. The complicated structure around PMTs is covered by the rings and plates.

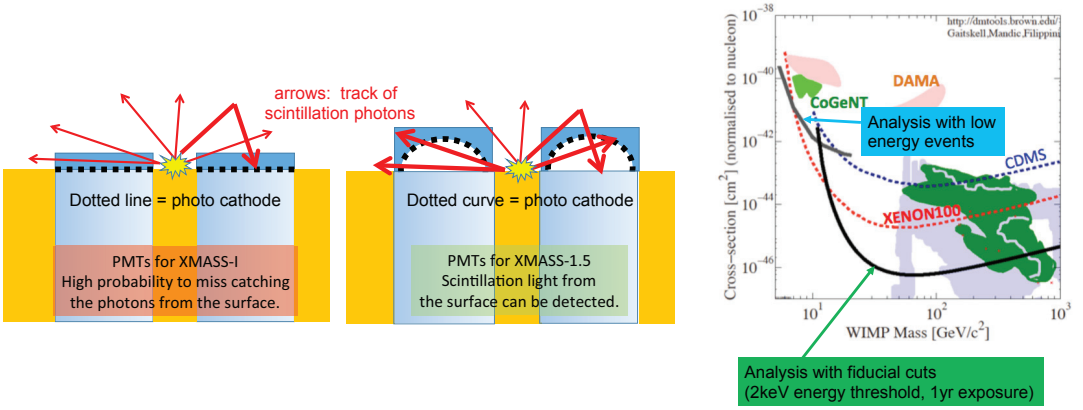

Fig. 7. (Left) Response to surface events of PMT with flat photocathode and a dome-shaped photocathode. Because the dome-shaped photocathode has a large acceptance for scintillation light from the inner surface of the detector, identification of surface events is much more efficient with the dome-shaped PMTs. (Right) Expected sensitivity with the XMASS-1.5 detector.

5. XMASS-1.5

We are planning to build a larger detector that will use five tons of liquid xenon, with one ton in the fiducial volume. To make a sensitive search for dark matter, we need to solve the problem related to surface events observed in the XMASS-I detector. We are designing dome-shaped PMTs as the key component to solve the problem. As shown in Fig. 7 (left), the problem arises because of a high probability for the flat photocathode to miss photons coming from scintillation at insensitive surface. However, the dome-shaped PMTs are more efficient for detecting them. In fact, our simulation shows that three PMTs surrounding the event vertices on the surface should detect 40%–50% of photoelectrons. This strongly indicates that reducing surface events is much easier and more reliable. With this improvement, we can search for heavy WIMPs with cross sections less than 10^{-46}cm^2. Figure 7 (right) shows the expected sensitivity of this detector. As for the axion-like particles, we expect a background reduction of two orders of magnitude. The XMASS-1.5 is a prototype of XMASS-2 and is expected to start in 2015.

6. Summary

The goal of the XMASS experiment is to directly detect dark matter using single-phase liquid xenon. The current-phase XMASS-I detector has the largest target mass (835 kg in total) and achieves the lowest energy threshold (300-eV-electron equivalent). The next phase detector, XMASS-1.5 is planned to start in 2015 and will have a total of five tons of liquid xenon. We discuss herein the results from XMASS-I (low-mass WIMPs, solar axions, annual modulation of event rate at low energy, and inelastic scattering of ^{129}Xe nuclei by WIMPs), the current status of hardware modifications of XMASS-I to reduce background, and progress in the design of XMASS-1.5.

References

[1] Y. Suzuki, arXiv:hep-ph/008296.
[2] K. Abe *et al.*, XMASS Collaboration, Astroparticle Physics 31 (2009) 290.
[3] K, Abe *et al.*, XMASS Collaboration, Nucl. Instr. Meth. A 661 (2012) 50.
[4] K. Abe *et al.*, XMASS Collaboration, Nucl. Instr. Meth. A 716 (2013) 78.
[5] K. Abe *et al.*, XMASS Collaboration, Phys. Lett. B 719 (2013) 78.
[6] K. Abe *et al.*, XMASS Collaboration, Phys. Lett. B 724 (2013) 46.
[7] K. Abe *et al.*, XMASS Collaboration, arXiv:1401.4737, submitted to PTEP.
[8] R. Bernabei *et al.*, New J. Phys. 2 (2000) 15.
[9] M. Pospelov, A. Ritz, and M. Voloshin, Phys. Rev. D 78 (2008) 115012.
[10] J. Redondo and M. Postma, JCAP 02 (2009) 005.